Cochran, J. R., Stow, D.A.V., et al., 1990
Proceedings of the Ocean Drilling Program, Scientific Results, Vol. 116

7. FISSION-TRACK ANALYSIS OF DETRITAL APATITES FROM SITES 717 AND 718, LEG 116, CENTRAL INDIAN OCEAN[1]

Jeff D. Corrigan[2] and Kevin D. Crowley[3]

ABSTRACT

This paper presents fission-track ages and confined track-length measurements from detrital apatites recovered from Ocean Drilling Program Leg 116 Site 717 and 718 cores. We interpret these data in terms of the post-depositional thermal history at these two sites and the thermotectonic history of apatite source areas. Composite apatite samples were derived by combining fine-grained sand samples from Sites 717 and 718 cores over 70- to 120-m intervals over the total depth penetrated at Sites 717 (T.D. = 820 mbsf) and 718 (T.D. = 960 mbsf). Thirty apatite grains per composite sample from ten samples (at least every other sampled interval) were dated and track-length measurements (20–50 per sample) were obtained for all samples.

Mean track lengths from Site 717 samples are statistically identical, ranging from 14.4 ± 0.4 to 14.8 ± 0.3 μm (all errors are the 95% confidence interval), and mean fission-track ages increase monotonically downhole from 4.8 ± 1.1 to 14.3 ± 2.3 Ma. For Site 718, located approximately 7 km to the south of Site 717 on an adjacent fault block, mean track lengths to 560 mbsf are equivalent to those measured from Site 717 samples. A decrease in mean track length (14.6 ± 0.3 to 13.2 ± 0.4 μm) and a corresponding decrease in mean fission-track age (21.1 ± 2.9 to 15.8 ± 2.4 Ma) with depth for samples between 560 and 960 mbsf from Site 718 indicates that post-depositional downhole shortening of fission tracks at elevated temperatures has taken place.

Track-length shortening, based on mean track lengths relative to an unannealed mean track length of 16.3 μm, is approximately 10% for all Site 717 samples and for samples from the upper 560 m of Site 718. The total amount of shortening of the lowermost sample from Site 718 is approximately 20%. Based on extrapolation of published laboratory annealing experiments, maximum isothermal time-temperature condition extremes that could produce this degree of annealing at the base of Site 718 are estimated to range from 50°C for a duration of 17 m.y. (since deposition) to 55°C for a duration of 7.5 m.y. (since the onset of deformation). These estimates argue against regional thermal conduction as the only mechanism for post-depositional heating and support seafloor heat flow and shipboard geochemical evidence for local convective heat transfer in the vicinity of Site 718.

In terms of source-area implications, dated samples have mean apatite fission-track ages that are only 0 to 10 m.y. older than depositional ages. These young ages imply rapid transport of sediment to the distal Bengal Fan and source areas characterized by high denundation rates (≤300 m/m.y.). These rates suggest that source areas similar to parts of the present-day Himalayas supplied sediment to the distal Bengal Fan since at least 17 Ma.

INTRODUCTION

Objectives

Fission-track analysis of detrital apatites recovered from Ocean Drilling Program (ODP) Leg 116 Sites 717 and 718 cores is used to: (1) constrain the thermal history of sediments overlying a region of deformed oceanic crust characterized by anomalous heat flow, and (2) characterize the thermotectonic history of the source terrane(s) from which the sediments originated.

A detailed heat-flow survey of the Leg 116 sites showed that heat flow over kilometer-scale distances in the vicinity of Site 718 ranged from 44 to 166 mW/m^2, providing strong evidence for upward migration of heat-carrying pore fluids (Cochran, Stow et al., 1989). Local convective heat transfer is also suggested by nonlinear temperature-depth profiles from other anomalous heat-flow areas in the central Indian Ocean (Geller et al., 1983). However, the heat source is unknown at this time. Anomalous heat flow in areas of the central Indian Ocean may be a consequence of lithospheric deformation evidenced by folding and faulting of the oceanic crust and overlying sediments (Weissel et al., 1980; Geller et al., 1983). To elucidate the origin of these heat-flow anomalies, Site 718 was drilled to collect downhole temperature, geochemical, and sediment physical property data.

The primary objective of this study is to constrain the thermal evolution of sediments recovered from Site 717 and 718 holes using apatite fission-track analysis. The age of oceanic crust in the vicinity of Leg 116 sites is estimated to be about 80 Ma (Norton and Sclater, 1979). The theoretical heat flow for 80 Ma crust is about 55 mW/m^2 (Parsons and Sclater, 1977). For steady-state conduction and a mean sediment thermal conductivity of 1.6 W/°C m, a geothermal gradient on the order of 35°C/km is required to maintain this heat flow through the seafloor. For a 35°C/km gradient and heating durations less than 17 Ma (the age of oldest sediment recovered from Leg 116 holes), the upper kilometer of sediment would not attain thermal conditions capable of appreciable shortening of fission tracks in apatite. Shortening of fission tracks that could unambiguously be attributed to post-depositional thermal conditions would, therefore, provide evidence for additional heating by some mechanism other than conduction.

The second objective of this study is to use apatite fission-track ages to provide information on distal Bengal Fan source areas. Combined, drilling at Sites 717 and 718 yielded 1470 m of distal Bengal Fan stratigraphy that records a near continuous history of sedimentation over the past 17 Ma (Cochran, Stow et al., 1989). To the extent that the Bengal Fan records the unroofing of the active Himalayan orogeny, apatite fission-

[1] Cochran, J. R., Stow, D.A.V., et al., 1990. *Proc. ODP, Sci. Results*, 116: College Station, TX (Ocean Drilling Program).
[2] Department of Geological Sciences, The University of Texas at Austin, Austin, TX 78713, U.S.A.
[3] Department of Geology, Miami University, Oxford, OH 45056, U.S.A.

track ages from these two sites provide a means of evaluating source-area denundation rates and the duration of time spent in transport by sediment deposited along the distal fan.

Apatite Fission-Track Analysis

Apatite fission-track analysis is a thermochronometric method that utilizes the annealing susceptibility of damage zones at low temperatures in this mineral to derive thermal history information. The spontaneous fission of trace amounts of ^{238}U in uranium-bearing minerals such as apatite produces two highly energetic fission fragments that create a linear trail of atomic defects (fission tracks) through the crystal lattice of these minerals (Fleischer et al., 1975). As the spontaneous fission rate of ^{238}U is statistically constant, the density of fission tracks in a mineral is a function of its uranium concentration and fission-track age. Fission-track ages record the minimum elapsed time during which tracks now present in the mineral have accumulated. Fission tracks in apatite anneal (shorten) at temperatures ranging from about 100°C to 400°C over short-term (<1 yr), laboratory time scales (Laslett et al., 1987). For most geologic situations, partial annealing of fission tracks in apatite occurs over a temperature range of 20°C to 150°C based on empirical data from drill core samples with well-constrained thermal histories (Gleadow and Duddy, 1981; Naeser, 1981). Naeser's (1981) data indicate that complete track annealing occurs over a temperature range of about 105°C to 150°C for heating durations of 10^8 to 10^5 yr, respectively.

Apatite fission-track analysis involves both the determination of fission-track ages and the measurement of confined fission-track lengths. For samples that have cooled rapidly through the zone of partial track stability, and have remained below the zone of partial track stability since cooling, the fission-track age is a minimum estimate of the time since the apatite passed through its closure temperature (Dodson, 1973). However, due to natural geologic heating, apatite fission-track ages may not correspond to any geologic "event." Information about the cooling history, such as cooling rate or post-cooling thermal pulses, is provided by the mean track length and the track-length distribution (Crowley, 1985; Gleadow et al., 1986; Duddy et al., 1988). In this study, variations in fission-track ages and track-length distributions with depth are used to constrain the post-depositional thermal histories at Sites 717 and 718.

METHODS

Sampling Procedure and Preparation

Samples from Leg 116, Site 717 and 718 holes, are used in this study. Samples were collected from the basal part of gray, fine-grained, sand-mud turbidite beds (Facies 1 of Cochran, Stow et al., 1989). Ten to fifteen, 10- to 20-cm^3 samples were combined over 70- to 120-m intervals starting from the base of each hole to provide sufficient material for analysis (Appendix A). A total of 14 composite samples, seven from each site, were collected (Fig. 1). Composite samples are denoted by the last digit of the hole (7 = hole at Site 717; 8 = hole at Site 718)

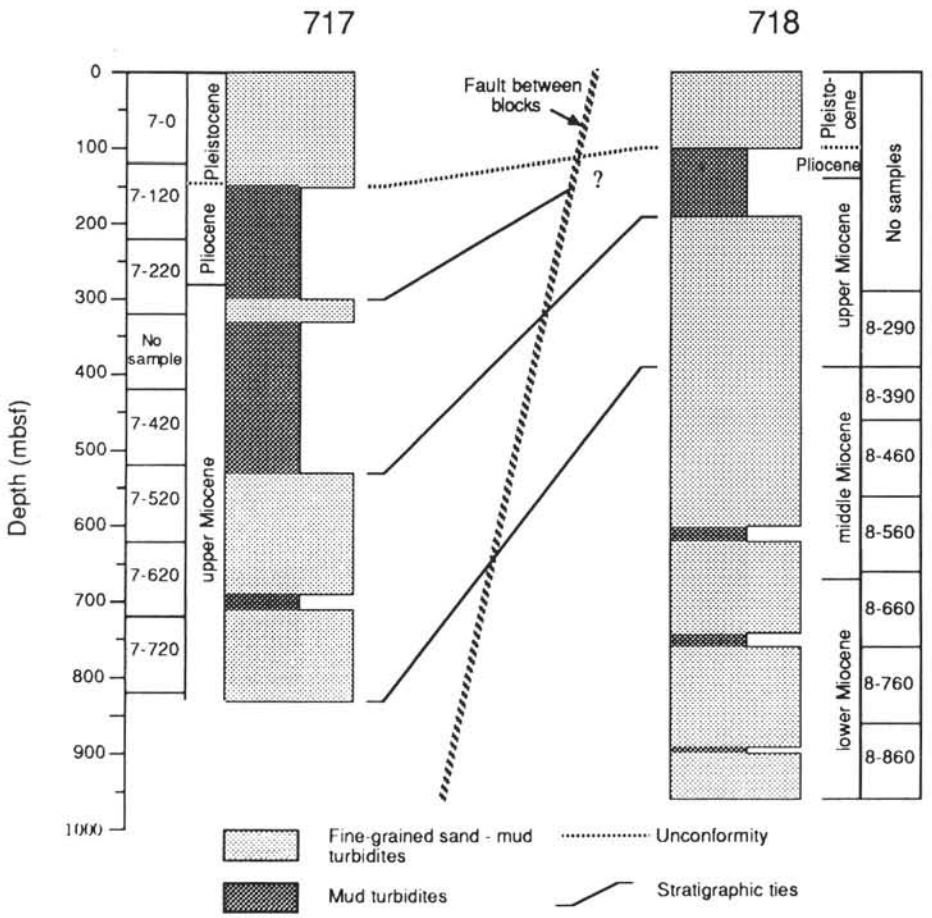

Figure 1. Generalized stratigraphic columns for holes at Sites 717 and 718 showing the sampled intervals for composite apatite samples (mbsf = meters below seafloor).

and the top of the collection interval in mbsf. For example, sample 7-660 is from sediment recovered at Site 717 and contains apatites from the 660 to 760 mbsf interval (Fig. 1, Table 1). Samples were wet-sieved to concentrate the fraction >63 μm. Apatite grains were further concentrated using standard heavy-liquid and magnetic-separation techniques. Apatite separates from each sample were split into two aliquots (one for track-length measurements and one for age determinations) and mounted in epoxy. The mounts were then ground with abrasives to expose internal grain surfaces, and polished using 0.3-μm aluminum oxide on a vibrating lap. Both mounts were etched in 7% HNO_3 (1.6 M) at 20°C for 40 s to reveal spontaneous tracks.

Analytical Procedures

One set of mounts was dated by the external detector method. These mounts were covered with low-uranium muscovite sheets and irradiated at the Texas A&M University reactor facility at a nominal thermal neutron fluence of 1×10^{16} neutrons/cm^2. Neutron fluences were monitored using National Bureau of Standards (NBS) SRM 612 glasses located at the middle and ends of the reactor tubes. After irradiation, muscovite covers on grain mounts were etched in 48% HF for 15 min at 25°C to reveal induced tracks. Muscovite covers on NBS glasses were etched in 48% HF for 45 min at 25°C. Muscovite covers on NBS glasses were counted with a 40× dry objective at a total magnification of 750×. Spontaneous and induced track counts were made using a 100× oil-immersion objective at a total magnification of 1875×.

Ages of individual apatite grains (Appendix B) were calculated using a zeta calibration (Hurford and Green, 1982, 1983) employing the Durango apatite (Naeser and Fleischer, 1975) as the age standard. A zeta calibration factor (Hurford and Green, 1983) for the age equation (Appendix B) was established for each of nine runs of the Durango apatite of known age (30.6 ± 0.6 Ma; Naeser and Fleischer, 1975). A weighted-mean of these zeta determinations of 322 ± 20 yr/(tracks·cm^{-2}) was then used to calculate fission-track ages. The error associated with this zeta determination is the standard error of the mean at the 95% confidence interval calculated by propagating Poisson errors for fossil track counts in the age standard, induced track counts in the mica detectors, and track counts in the fluence monitors, as well as the uncertainty in the age of the standard.

To reduce the possibility of bias in individual age determinations, the first 30 *countable* grains encountered in the mounts were dated. Countable grains were defined as those (1) oriented with their *c*-axes parallel or subparallel to the polished mount surface and (2) devoid of numerous defects (cracks, inclusions and/or dislocations). A key point in this procedure is that grains with low track densities were not avoided if otherwise appropriate for counting. Ages reported in the text and figures are mean (pooled) ages. Uncertainties in individual and mean fission-track ages were calculated by propagating Poisson errors for fossil track counts, induced track counts, and track counts in the fluence monitors, as well as systematic errors arising from uncertainties in the zeta calibration factor. Uncertainties in ages given in the text and figures represent the standard error of the mean at the 95% confidence interval.

The lengths of horizontal, confined spontaneous tracks in prismatic sections from the second, unirradiated set of mounts were measured with the oil-immersion lens at 1875× using a drawing tube and digitizing pad. For samples containing grains with sufficient track densities, the lengths of 50 confined, horizontal tracks were measured from the set of unirradiated mounts. Due to uphole decreases in spontaneous track density, fewer confined track-length measurements are available for samples with a depositional age of less then 10 Ma (Table 1). Uncertainties in sample mean track length also represent the standard error of the mean at the 95% confidence interval.

RESULTS

Confined Track Lengths

Mean lengths of horizontal, confined spontaneous tracks from Site 717 samples are identical, within error, and range from 14.4 ± 0.5 to 14.8 ± 0.3 μm (Fig. 2A). These mean lengths are about 10% shorter than mean lengths of unannealed, induced tracks in apatite, which are about 16.3 μm (Gleadow et al., 1986). Mean confined track lengths from the upper part of the section at Site 718 (290–560 mbsf) are also identical within error (Fig. 2B), and they are statistically indistinguishable from Site 717 sample mean lengths (Table 1).

Table 1. Data summary for samples from holes at Sites 717 and 718.

Sample*	Average Depth (mbsf)	Depth Range (mbsf)	Average Depositional Age (Ma)**	Depositional Age Range (m.y.)**	Mean AFT^ Age (m.y.)	95% C.I. (m.y.)	Mean Track Length (μm)	95% C.I. (μm)	Number Tracks Measured
7-0	60	0-120	0.3	0.0?-0.6	4.8	1.1	14.6	0.5	20
7-120	170	120-220	1.4	0.6-2.2	-	-	14.4	0.5	20
7-220	270	220-320	3.0	2.2-3.8	6.7	1.6	14.5	0.4	26
7-420	470	420-520	6.0	5.6-6.3	9.0	1.6	14.5	0.4	25
7-520	570	520-620	6.9	6.3-7.5	-	-	14.6	0.3	40
7-620	670	620-720	8.0	7.5-8.5	11.9	2.0	14.8	0.3	25
7-720	770	720-820	9.0	8.5-9.5	14.3	2.2	14.6	0.5	27
8-290	340	290-390	9.0	8.4-9.7	16.2	2.3	14.8	0.4	40
8-390	425	390-460	10.0	9.7-10.3	-	-	14.7	0.4	35
8-460	510	460-560	10.6	10.3-10.8	21.1	2.9	14.6	0.3	39
8-560	610	560-660	11.9	10.8-13.0	-	-	14.2	0.3	50
8-660	710	660-760	14.4	13.0-15.7	18.4	2.6	14.2	0.3	50
8-760	810	760-860	16.3	15.7-16.8	18.5	3.0	13.9	0.4	50
8-860	910	860-960	17.0	16.8-17.2	15.8	2.4	13.2	0.4	50

* First digit of sample number corresponds to last digit of hole number (7 = Site 717, 8 = Site 718).
** Based on linear interpolation between biostratigraphic age assignments (Cochran, Stow et al., 1989).
^ AFT - apatite fission-track.

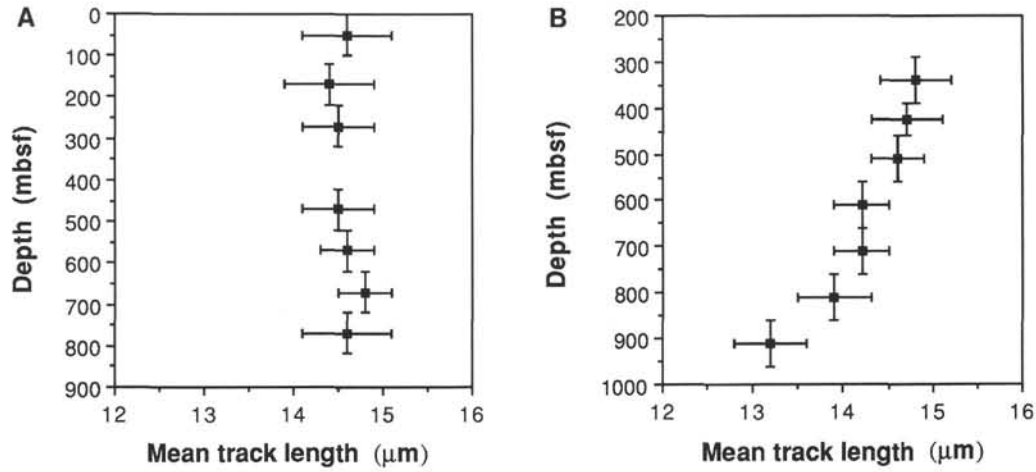

Figure 2. Downhole plots of mean track length for **A.** Site 717 and **B.** Site 718. The vertical bars indicate the depth intervals of composite apatite samples. The horizontal bars are the standard error of the mean at the 95% confidence interval.

Mean confined track lengths decrease from 14.2 ± 0.3 μm below 560 mbsf to 13.2 ± 0.4 μm at the base of the hole (Fig. 2B). Apatites from the lowermost sample (860–960 mbsf) have a mean confined track length that is 20% shorter than that observed for unannealed induced fission tracks in apatite. Track-length distributions for individual samples from both sites are unimodal with one sigma standard deviations ranging from 0.9 to 1.4 μm (Fig. 3).

Fission-Track Ages

Mean fission-track ages from Site 717 samples increase monotonically from 4.8 ± 1.1 Ma at the top of the hole to 14.3 ± 2.2 Ma at the base (Fig. 4A). These ages are on the order of 3 to 5 m.y. older than the sediment depositional ages (Fig. 4A). Mean fission-track ages for the two dated samples in the upper parts of holes at Site 718 increase with depth (Fig. 4B). The uppermost sample from Site 718 (8-290) and lowermost sample from Site 717 (7-720) are derived from equivalent stratigraphic intervals (Fig. 1). These samples give mean fission-track ages of 16.2 ± 2.3 Ma and 14.3 ± 2.2 Ma, respectively, and provide a check on the consistency of the data. Mean fission-track ages below 560 mbsf at Site 718 show an overall decrease in age with depth (Fig. 4B). The lowermost sample (8-860) has a mean fission-track age that is less than or equal to the average depositional age (Fig. 4B). Although these samples are composed of detrital grains, histograms of single grain ages are unimodal (Fig. 5). The variance of single-grain ages about the mean age is on the order of 10 to 40 m.y. for all samples except 8-460, which contains one outlier (Fig. 5).

INTERPRETATION

Post-Depositional Thermal Histories of Sites 717 and 718

Statistically constant mean track lengths that are only about 10% shorter than unannealed, induced track lengths observed in samples from Site 717 (Fig. 2A), coupled with the monotonic increase in mean fission-track ages with depth (Fig. 4A), indicate that these samples have existed at ambient or near-ambient temperatures since deposition. Studies of confined track lengths in apatites from a variety of geological settings indicate that, even in undisturbed volcanic rocks that cooled rapidly and were subjected to post-cooling temperatures of less than about 50°C, spontaneous track lengths are always shorter than induced track lengths (Gleadow et al., 1986). These observations indicate that fission-track lengths in apatite are unstable even at ambient temperatures (Green, 1980, 1988). Hence, the 10% shortening observed in Site 717 samples may be explained in large part by their annealing at ambient temperatures.

The systematic decrease in mean track length and age with depth below 560 mbsf at Site 718 (Figs. 2B and 4B) indicates post-depositional shortening of tracks has occurred over this interval. Recent laboratory annealing studies of apatite confirm earlier observations suggesting that increased chlorine content in the anion site corresponds to an increased resistance to track shortening at any given temperature (Green et al., 1985; Crowley and Cameron, unpubl. data). Electron microprobe-derived compositional data on apatites from Site 717 and 718 samples (Appendix C) indicate that apatite chlorine content does not vary appreciably between samples. Thus, it is unlikely that the observed downhole shortening of track lengths is related to differences in apatite chemistry. Of the approximately 20% total shortening of mean track length observed in sample 8-860 from the base of the recovered section at Site 718, we estimate that approximately 10% is due to annealing at ambient conditions (as discussed above) and the remaining 10% is due to post-depositional annealing at elevated temperatures.

To constrain time-temperature conditions that could produce the 20% total track-length shortening observed at the base of the recovered section at Site 718, we use Laslett et al.'s (1987) extrapolation of their experimental track-length annealing studies on unannealed induced fission tracks in Durango apatite. There are several difficulties with this approach. First, uncertainties regarding modeling of annealing data are compounded when they are extrapolated several orders of magnitude to geologic time scales (Laslett et al., 1987). Second, annealing resistance in apatite is known to vary with apatite composition, with chlorine varieties being most resistant (Green et al., 1985; Crowley and Cameron, unpubl. data). Compositional data indicate that most apatites analyzed in this study are F-OH apatites (chlorine atoms per 13 oxygens < 0.03), whereas the Durango apatite is a F-Cl apatite (chlorine atoms per 13 oxygens = 0.08; Young et al., 1969). Thus, extrapolation of track-length annealing data from Durango apatite may overestimate temperatures required to produce an equivalent amount of fission-track shortening in these samples. Finally, Laslett et al. (1987) investigated annealing for isothermal conditions, whereas variable temperature

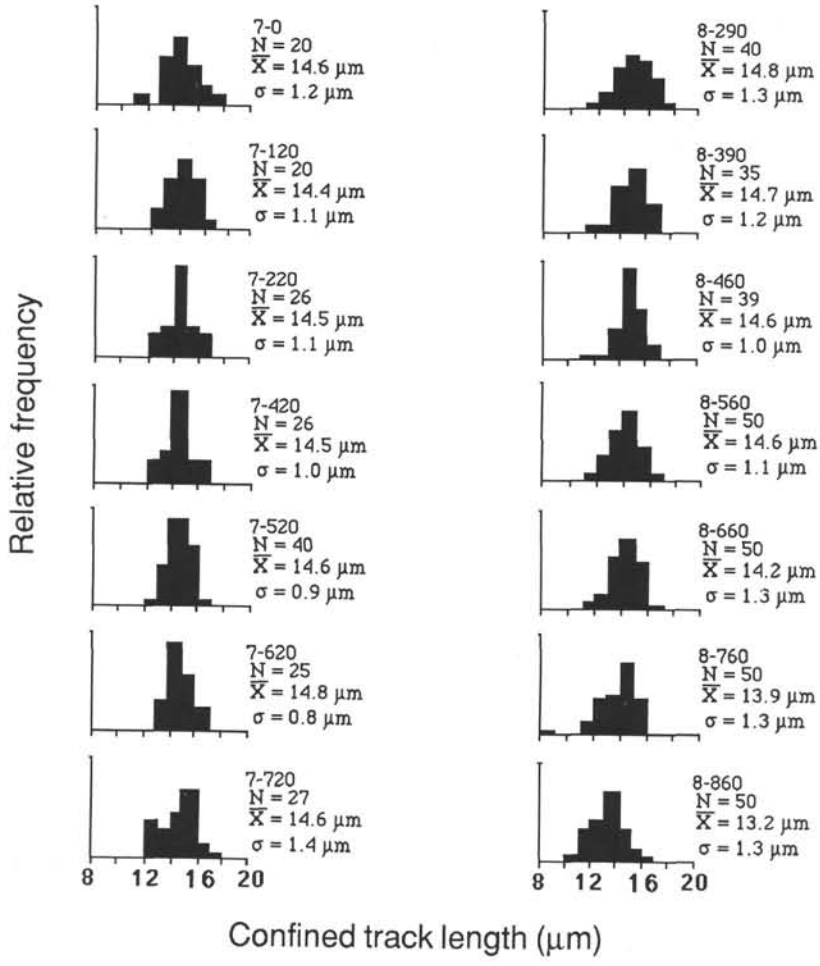

Figure 3. Histograms of confined track-length measurements over 1.0-μm intervals. Sample number, number of track lengths measured (N), mean track length ($\bar{x}$), and one-sigma standard deviation (σ) are given for each plot.

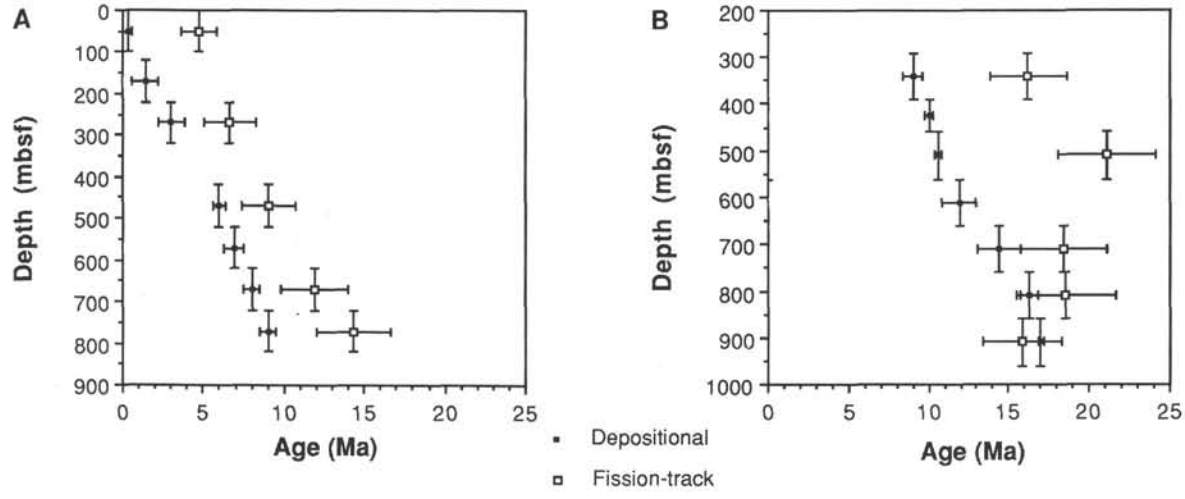

Figure 4. Downhole plots of sample average depositional ages and mean fission-track ages for **A.** Site 717 and **B.** Site 718. The vertical bars indicate the depth intervals of composite apatite samples. The horizontal bars on depositional ages give the range of depositional ages for samples. The horizontal bars on mean fission-track ages are the standard error of the mean at the 95% confidence interval.

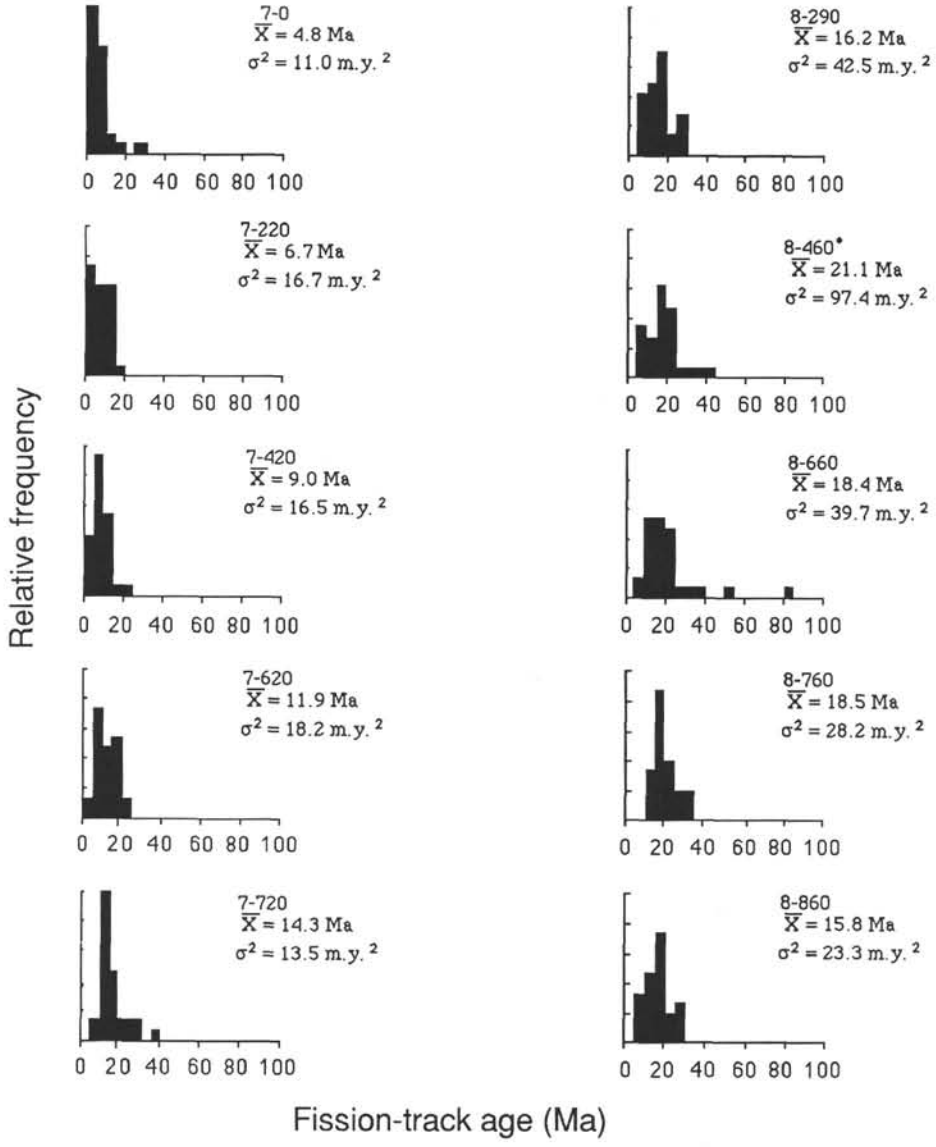

Figure 5. Histograms of fission-track ages for dated samples over 5-m.y. intervals. Sample number, mean age ($\bar{x}$), and variance (σ^2) of individual ages about the mean age are given for each plot. *—one grain with an age of 190.3 ± 79.0 Ma plots off the scale of the graph. Note that single-grain ages and their associated uncertainties are about the same order of magnitude (Appendix B).

annealing is expected for geologic settings. With these limitations in mind, we use Laslett et al.'s (1987) preferred fanning model to estimate that isothermal time-temperature conditions capable of producing a track-length reduction from 10% to 20% in the lowermost sample from Site 718 range from 50° to 55°C, for durations ranging from 17 m.y. (since deposition) to 7.5 m.y. (since the onset of faulting), respectively (Fig. 6).

Sediments at the base of the drilled section at Site 718 have been within about 100 m of their present depth below seafloor since the onset of deformation (7 Ma). For a predicted conductive heat flow of 55 mW/m² for the approximately 80-m.y.-old crust beneath Leg 116 sites (Parsons and Sclater, 1977; Norton and Sclater, 1979), and average, measured, sediment thermal conductivities of 1.3 W/°C m above 200 mbsf and 1.9 W/°C m below 200 mbsf (Cochran, Stow et al., 1989), a present-day temperature of 33°C is predicted at a depth of 960 mbsf at Site 718 for purely conductive heat transfer assuming steady-state conditions. Apatite fission-track data presented here provide evidence for temperatures greater than 50°C at depths of 860 to 960 mbsf at Site 718, indicating that conductive heat transfer due to lithospheric cooling cannot account for the observed track shortening in samples below 560 mbsf at Site 718.

Variable and anomalously high heat-flow values in the vicinity of Site 718 suggest advection of heat via upward migration of pore fluids (Cochran, Stow et al., 1989). Shortening of fission tracks in apatite at elevated temperatures below 560 mbsf at Site 718 implies that convective heat transfer, as evidenced by seafloor heat-flow data in the vicinity of Site 718, is not a transient phenomenon. No evidence is found from either downhole temperature or fission-track data for hydrothermal activity near Site 717, located just 7 km north of Site 718 on an adjacent fault block. The fault separating these two blocks is located approximately 1.5 km north of Site 718 and has been active since 7.5 Ma (Cochran, Stow et al., 1989). The heat flow conclusions and fission-track

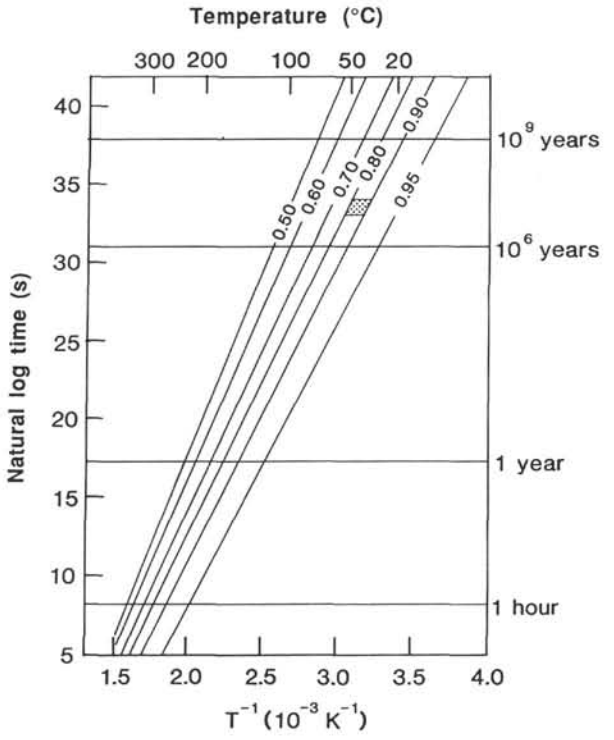

Figure 6. Fanning Arrehnius diagram for experimental apatite fission-track-length annealing data of Laslett et al. (1987) extrapolated to geologic time scales. The shaded region indicates the range of isothermal time-temperature conditions capable of producing track shortening observed in the lowermost sample (8-860) from Site 718.

observations from Site 718 suggest that this fault provides a conduit for upward migration of heated pore fluids.

Bengal Fan Source Areas

A first-order observation from Figure 4 is that mean fission-track ages of samples from Sites 717 and 718 do not deviate from the average depositional age of these apatites by more than about 10 m.y. Because Durango apatite, used in the zeta calibration for calculating fission-track ages, has a mean track length that is 9% shorter than unannealed, induced tracks (Gleadow et al., 1986), we implicitly correct for equivalent amounts of track shortening in calculating fission-track ages for samples in this study. For samples from Site 717 and the upper part of Site 718, which have experienced ≤10% track shortening, the last significant cooling event occurred within about 3 to 10.5 m.y. prior to deposition. Cerveny et al. (1988) obtained very similar results in their fission-track study of detrital zircons from Siwalik Group sandstones and Indus River sands in northern Pakistan. They found that these fluvial sands and sandstones contain zircons that are only 1 –5 m.y. older than sample depositional ages (≤18 Ma).

Continuous volcanism throughout the Neogene in the source area(s) could explain such young fission-track ages in detrital apatites from the distal Bengal Fan. However, Neogene volcanics in possible source areas on the Indo-Eurasia continent are really restricted (Gansser, 1964). The most extensive area of young volcanism appears to be the Gangdese (Trans-Himalayan) Belt, southern Tibet, where *local* activity has been placed around 10–15 Ma (Coulon et al., 1986). Crystallization ages of exposed batholiths in the Gandese Belt range from 110 to 40 Ma (Schrärer et al., 1984; Xu et al., 1985), and the timing of major volcanic activity in this region is placed around 50–60 Ma (Coulon et al., 1986). The timing of this magmatic activity is too early to account for the apatite ages found in samples from Sites 717 and 718. A more likely explanation for these ages is that they record the timing of rock uplift in the source area(s) through the zone of partial track stability for apatite.

A detrital apatite fission-track age represents the elapsed time during which tracks have accumulated; the age records contributions from its uplift, transport, and post-depositional histories. In the case where no post-depositional annealing has affected the age, the observed age, t_{obs}, is given by:

$$t_{obs} = t_u + t_t + t_s \quad (1)$$

where: t_u = elapsed time required for apatite to pass through its effective closure temperature (110 ± 10°C) and reach the surface (a function of uplift *and* erosion), t_t = elapsed time spent in transport, and t_s = elapsed time since final deposition (Zeitler et al., 1986). The elapsed time since final deposition, t_s, can be estimated from nannofossil biostratigraphy (Table 1 and Cochran, Stow et al., 1989). Because post-depositional track shortening is implicitly corrected for by using an age standard with a similar amount of track shortening for samples from Site 717 and Site 718, taking the mean fission-track age for these samples to be T_{obs} provides a minimum estimate of the timing of the last significant cooling event. If rates of erosion kept pace with rates of uplift, a reasonable first-order approximation, t_u can be interpreted as the elapsed uplift time. Therefore, the averaged combined time that apatites spent in uplift (after passing through their closure temperature) and transport for a given sample is estimated by $t_{obs} - t_s$ (Fig. 7). If it is assumed that $t_u = 0$, these time intervals also provide an upper limit on the sample-averaged sediment transport time, indicating that sediment spent no more than about 10 m.y. reaching the distal Bengal Fan after leaving their source areas. Similarly, taking transport time to be effectively instantaneous (setting $t_t = 0$) provides an estimate of maximum, sample-averaged elapsed uplift time. Maximum, sample-averaged

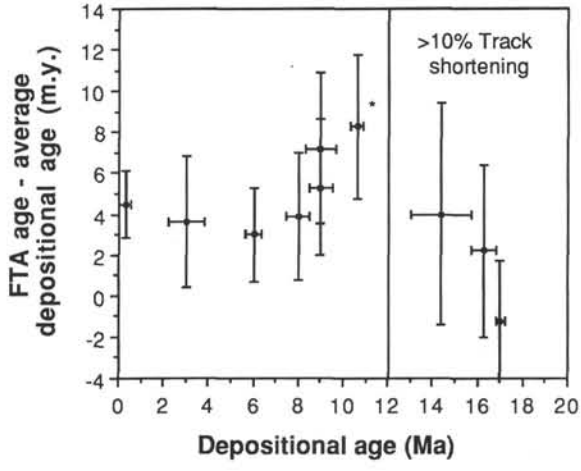

Figure 7. Mean fission-track age minus the average depositional age plotted against average depositional age (*—based on a mean age of 18.9 ± 2.7 Ma for sample 8-460 determined by not including the single-grain age of 190.3 ± 79.0 Ma). Mean age minus average depositional age provides a sample-averaged estimate of the maximum duration of time spent in transport, as well as a sample-averaged estimate of the maximum duration of time required for apatite to reach the surface after passing through its effective closure temperature (110° ± 10°C). See text for assumptions and derivation of estimates.

elapsed uplift times determined in this manner range from 2 to 9 m.y. for samples with ≤10% track shortening (Fig. 7).

These maximum, sample-averaged elapsed uplift times provide a basis for estimating source area denundation rates. Neglecting radiogenic heat production and assuming (1) a constant source-area geothermal gradient, (2) apatites passed upward through stationary isotherms (relative to the earth's surface), and (3) erosion rates approximated uplift rates, an estimate of the minimum, sample-averaged denundation rate (dz/dt_{min}) is given by:

$$dz/dt_{min} = \frac{T_{eff}}{(dT/dz)\ (t_{umax})} \quad (2)$$

where T_{eff} = the effective closure temperature of the apatite fission-track system (110° ± 10°C), dT/dz = the average geothermal gradient in the source area, and t_{umax} = the maximum, sample-averaged uplift time as defined above. Taking 30°C/km is an appropriate geothermal gradient for an orogenic terrane (Blackwell, 1971) gives sample-averaged, minimum denundation rates on the order of 0.5 to 1.5 km/m.y. However, these estimates invalidate assumptions (1) and (2). Denundation rates approaching or exceeding about 300 m/m.y. will compress near-surface isotherms, causing a corresponding increase in geothermal gradients (Parrish, 1985; Koons, 1987). The above estimates would therefore overestimate true uplift rates. On the other hand, if we assume source area, upper-crustal geothermal gradients never exceeded 60°C/km, which we take as a reasonable upper limit, then these data still imply source-area denundation rates of ≥300 m/m.y. for all samples. Zeitler et al. (1986) inferred similar unroofing rates for parts of the northern Pakistan Siwalik Group source areas from fission-track ages of detrital zircons contained in Siwalik Group sandstones.

CONCLUSIONS

Fission-track ages and confined track-length measurements from detrital apatites recovered from Leg 116 cores obtained from Sites 717 and 718 constrain the thermal history of the sediments at these two sites and the thermotectonic histories of their source areas. Statistically-constant mean track lengths observed from Site 717 samples suggest that downhole temperatures have never exceeded about 50°C. A decrease in mean track length (14.6 ± 0.3 to 13.2 ± 0.4 μm) and mean fission-track age (21.1 ± 2.9 to 15.8 ± 2.4 Ma) with depth from 560 to 960 mbsf at Site 718 indicates post-depositional shortening of fission tracks at elevated temperatures below 560 mbsf. The total amount of track shortening is estimated to be approximately 20% for the lowermost sample (860- to 960-msbf interval) at Site 718. Based on extrapolation of published laboratory track-length annealing experiments, isothermal time-temperature condition extremes that could produce this degree of shortening are estimated to range from 50°C for 17 m.y. (since deposition) to 55°C for 7.5 m.y. (since the onset of faulting). These estimates argue against conductive heating due to lithospheric cooling as the only mechanism for heating and suggest an additional heat source and/or heat transport mechanism near Site 718.

Dated samples have mean ages that are between 0 and 10 m.y. older than depositional ages. These young ages indicate that sediment transport from source areas required no more than about 10 m.y. Such young cooling ages for detrital apatites also imply source areas characterized by high uplift and erosion rates (≥300 M/m.y.). These denundation rates suggest that source areas similar to parts of the present-day Himalayas supplied sediment to the distal Bengal Fan since at least 17 Ma.

ACKNOWLEDGMENTS

This investigation was stimulated by a seminar taught by Mark Cloos. We also thank John Krohn of Texas A&M University for conducting sample irradiations, Dwight Deuring of Southern Methodist University for assistance in running some of the electron microprobe analyses, as well as the U.S. Department of Energy for support provided through the Reactor-Sharing Program at Texas A&M University. Critical reviews by Mark Cloos and Charles W. Naeser improved this manuscript. Funding for this study was provided by a JOI/USSAC Ocean Drilling Program Fellowship and a University of Texas at Austin Institute for Geophysics Ewing-Worzel Fellowship to Corrigan.

REFERENCES

Bevington, P. R., 1969. *Data reduction and error analysis for the physical sciences*: New York (McGraw-Hill).

Blackwell, D. D., 1971. The thermal structure of the continental crust. *In* Heacock, J. G. (Ed.), *The Structure and Physical Properties of the Earth's Crust*: Am. Geophys. Union Geophysical Monographs, 14:169–184.

Cerveny, P. F., Naeser, N. D., Zeitler, P. K., Naeser, C. W., and Johnson, N. M., 1988. History of uplift and relief of the Himalaya during the past 18 million years: Evidence from fission-track ages of detrital zircons from sandstones of the Siwalik Group. *In* Kleinspehn, K. L., and Paola C. (Eds.), *New Perspectives in Basin Analysis*: New York (Springer-Veriag), 43–61.

Cochran, J. R, Stow, D.A.V., et al., 1989. *Proc. ODP, Init. Repts.*, 116: College Station, TX (Ocean Drilling Program).

Coulon, C., Maluski, H., Bollinger, C., and Wang, S., 1986. Mesozoic and Cenozoic volcanics from central and southern Tibet: ^{39}Ar-^{40}Ar dating, petrological characteristics, and geodynamical significance. *Earth Planet.Sci. Lett.*, 79:281–302.

Crowley, K. D., 1985. Thermal significance of fission-track length distributions. *Nucl. Tracks*, 10:311–322.

Dodson, M., 1973. Closure temperature in cooling geochronological and petrological systems. *Contrib. Mineral. Petrol.*, 40:259–274.

Duddy, I. R., Green, P. F., and Laslett, G. M., 1988. Thermal annealing of fission tracks in apatite—3. Variable temperature behavior. *Chem. Geol. (Isotope Geoscience Section)*, 73:25–38.

Fleischer, R. L., Price, P. B., and Walker, R. M., 1975. *Nuclear Tracks in Solids:* Berkeley (University of California Press). Galbraith, R., 1980. On statistical models for fission track counts. *Math. Geol.*, 13:471–478.

Gansser, A., 1964. *The Geology of the Himalayas:* New York (Wiley-Interscience).

Geller, C. A., Weissel, J. K., and Anderson, R. N., 1983. Heat transfer and intraplate deformation in the central Indian Ocean. *J. Geophys. Res.*, 88:1018–1032.

Gleadow, A.J.W., and Duddy, I. R., 1981. A natural long-term annealing experiment for apatite. *Nucl. Tracks*, 5:169–174.

Gleadow, A.J.W., Duddy, I. R., Green, P. F., and Lovering, J. F., 1986. Confined track lengths in apatite—a diagnostic tool for thermal history analysis. *Contrib. Mineral. Petrol.*, 94:405–415.

Green, P. F., 1980. On the cause of shortening of spontaneous fission tracks in certain minerals. *Nucl. Tracks*, 4:91–100.

Green, P. F., 1981. A new look at statistics in fission-track dating. *Nucl. Tracks*, 5:77–86.

Green, P. F., 1988. The relationship between track shortening and fission track age reduction in apatite: combined influences of inherent instability, annealing anisotropy, length bias and system calibration. *Earth Planet. Sci. Lett.*, 89:335–352.

Green, P. F., Duddy, I. R., Gleadow, A.J.W., Tingate, P. R., and Laslett, G. M., 1985. Fission-track annealing in apatite: track length measurements and the form of the Arrhenius plot. *Nucl. Tracks*, 10:323–328.

Hurford, A. J., and Green, P. F., 1982. A user's guide to fission-track dating calibration. *Earth Planet. Sci. Lett.*, 59:343–354.

Hurford, A. J., and Green, P. F., 1983. The zeta age calibration of fission track dating. *Chem. Geol. (Isotope Geoscience Section)*, 1:285–317.

Koons, P. O., 1987. Some thermal and mechanical consequences of rapid uplift: an example from the Southern Alps, New Zealand. *Earth Planet. Sci. Lett.*, 86: 307–319.

Laslett, G. M., Green, P. F., Duddy, I. R., and Gleadow, A.J.W., 1987. Thermal annealing of fission tracks in apatite—2. a quantitative analysis. *Chem. Geol.*, 65:1–15.

Naeser, C. W., 1981. The fading of fission tracks in the geologic environment—data from deep drill holes. *Nucl. Tracks*, 5:248–250 (abstract). Naeser, C. W., and Fleischer, R. L., 1975. Age of the apatite at Cerro de Mercado, Mexico: a problem for fission track annealing corrections. *Geophys. Res. Lett.*, 2:67–70.

Norton, I. O., and Sclater, J. G., 1979. A model for the evolution of the Indian Ocean and the breakup with Gondwanaland. *J. Geophys. Res.*, 84:6803–6830.

Parrish, R. R., 1985. Some cautions which should be exercised when interpreting fission-track and other dates with regard to uplift calculations *Nucl. Tracks*, 10:425.

Parsons, B. and Sclater, J. G., 1977. An analysis of variation of oceanic floor bathymetry and heat flow with age. *J. Geophys. Res.*, 82:803–827.

Schrärer, U., Xu, R.-H., and Allégre, 1984. U-Pb geochronology of the Gandese (Transhimalaya) plutonism in the Lhasa-Xigaze region, Tibet. *Earth Planet. Sci. Lett.*, 69:311–320.

Weissel, J. K., Anderson, R. N., and Geller, C. A., 1980. Deformation of the Indo-Australian Plate. *Nature*, 287:284–291.

Xu, R.-H., Schräer, U., and Allégre, 1985. Magmatism and metamorphism in the Lhasa block (Tibet). *J. Geol.*, 93:41–57.

Young, E. J., Myers, A. T., Munson, E. L., and Conklin, N. M., 1969. Mineralogy and geochemistry of fluorapatite from Cerro de Mercado, Durango, Mexico. *U.S. Geol. Surv. Prof. Pap.*, 650-D:D84–D93.

Zeitler, P. K., Johnson, N. M., Briggs, N. D., and Naeser, C. W., 1986. Uplift history of the NW Himalaya as recorded by fission-track ages on detrital Siwalik zircons. *In* Jiqing, H. (Ed.), *Proc. Symp. Mesozoic and Cenozoic Geol.*, (60th anniv. meet., Geol. Soc. China): Beijing (Geological Publishing House): 48:1–494.

Date of initial receipt: 24 February 1989
Date of acceptance: 3 January 1990
Ms 116B-118

APPENDIX A

Sample Information

Composite samples used in this study consist of six to ten, 10- or 20-cm^3 shipboard core samples combined over 100-m intervals (except 7-0 and 8-390 which were sampled over 120- and 70-m intervals, respectively) beginning at the bases of holes at Sites 717 and 718. Shipboard sampling of these intervals was aimed at uniform representation of the entire interval. However, core recovery and the distribution of units containing sand ultimately dictated sampling. Insufficient recovery and/or lack of fine-grained sand from the 320 to 420 mbsf interval at Site 717 and the 0- to 290-mbsf interval at Site 718 prevented collection of composite apatite samples from these intervals (Fig. 1).

A summary of the composite samples is provided in the following tables. The depositional age range shown in the AGE column is based on a linear interpolation of age as a function of depth between the age assignments based on nannofossil zones (Cochran, Stow, et al., 1989). Ages with an asterisk (*) denote interpolated ages.

SAMPLE#	SITE	SAMPLES	DEPTH (mbsl)	VOLUME (cc)	INITIAL DRY WEIGHT (g)	>63 um WEIGHT (g)	NANNOFOSSIL ZONE	DEPOSITIONAL AGE (Ma)
717-0	717B,C		0-100	190	300	172	CN15-CN14a	0?-0.56*
	717B	2H-04-130-135	9.80	20				<0.5
	717B	2H-05-130-134	11.30	20				
	717C	2H-02-100-105	16.00	20				
	717C	4X-0S-2-6	31.52	20				
	717C	5X-02-28-32	42.78	20				
	717C	6X-02-31-33	47.81	10				
	717C	6X-02-35-37	47.85	10				
	717C	7X-CC-20-24	57.60	20				
	717C	8X-01-63-65	65.63	10				
	717C	10X-CC-15-20	76.15	20				
	717C	12X-CC-0-5	93.50	20				0.56*
717-120	717C		120-220	150	240	130	CN14-CN12	0.56*-2.2
	717C	16X-CC-16-21	123.46	20				
	717C	18X-CC-PALEO	131.63	10				
	717C	18X-CC-13-17	131.63	20				
	717C	19X-1-76-80	141.76	20				
	717C	20X-1-85-90	151.35	20				
	717C	22X-4-144-149	175.44	20				
	717C	23X-2-145-150	181.95	20				
	717C	26X-4-97-102	212.97	20				
717-220	717C		220-320	180	200	60	CN12a-CN11	2.2-3.8*
	717C	33X-CC-PALEO	283.60	30				
	717C	33X-CC-27-33	283.60	20				
	717C	34X-1-83-88	284.33	20				
	717C	34X-2-145-150	286.45	20				
	717C	36X-CC-PALEO	312.10	30				
	717C	36X-CC-27-32	312.10	20				
	717C	37X-2-106-111	314.56	20				
	717C	37X-CC-26-31	316.06	20				

Appendix A (continued).

SAMPLE#	SITE	SAMPLES	DEPTH (mbsl)	VOLUME (cc)	INITIAL DRY WEIGHT (g)	>63 um WEIGHT (g)	NANNOFOSSIL ZONE	DEPOSITIONAL AGE (Ma)
717-420	717C		420-520	170	340	75	CN9b-CN9	5.6-6.3*
	717C	51X-2-82-87	447.32	20				
	717C	51X-2-98-103	447.48	20				
	717C	53X-1-100-120	465.00	10				
	717C	53X-1-117-121	465.17	20				
	717C	57X-4-80-85	507.30	50				
	717C	57X-4-104-109	507.54	50				
717-520	717C		520-620	210	410	135	CN9-CN9	6.3*-7.5*
	717C	60X-3-61-63	534.11	10				
	717C	61X-1-107-11	541.07	20				
	717C	62X-1-15-19	549.65	20				
	717C	62X-CC-6-10	550.42	20				
	717C	63X-1-33-38	559.33	20				
	717C	64X-3-146-151	572.96	20				
	717C	64X-4-1-3	573.01	10				
	717C	67X-1-108-112	598.08	20				
	717C	67X-2-77-81	599.27	20				
	717C	68X-4-145-150	611-63	20				
	717C	69X-1-10-14	616.10	10				
	717C	69X-1-14-19	616.14	20				
717-620	717C		620-720	260	535	165	CN9-CN8b	7.5*-8.5*
	717C	69X-CC-21-26	620.31	20				
	717C	71X-4-100-106	640.50	40				
	717C	71X-5-90-95	641.90	20				
	717C	72X-1-64-70	645.14	40				
	717C	74X-1-94-100	664.44	40				
	717C	75X-4-35-40	677.85	20				
	717C	75X-CC-33-38	678.30	20				
	717C	76X-3-83-88	686.33	20				
	717C	78X-6-128-132	710.20	20				
	717C	79X-3-61-66	714.61	20				
717-720	717C		720-820	260	535	147	CN8b-CN7?	8.5*-9.5
	717C	80X-03-39-45	723.89	40			CN8b	
	717C	81X-CC-24-28	731.12	20				
	717C	82X-01-29-35	739.50	40				
	717C	83X-01-74-80	749.74	40				
	717C	84X-03-95-100	762.45	20			CN8?	
	717C	85X-02-98-104	770.48	40				
	717C	86X-CC-9-14	777.89	20				
	717C	87X-01-61-66	787.61	20				
	717C	88X-01-68-73	797.18	20			CN7?	9.2*
718-190	718C		190-290	100	150	50	CN9-CN9	??-8.4?
	717C	25X-1-106-111	238.36	20				
	717C	25X-2-8-13	238.88	20				
	717C	26X-2-21-26	248.50	20				
	717C	27X-CC-19-23	257.61	20				
	717C	29X-1-70-75	276.00	20				
718-290	718C		290-390	90+	260	92	CN9-CN7?	8.4*-10.0
	718C	32X-01-132-134	305.12	10			CN9	8.5*
	718C	33X-CC-10-15	313.63	20				
	718C	36X-CC-22-27	343.42	20				
	718C	38X-01-72-77	361.52	20				
	718C	40X-CC-5-10	380.41	20				
	718C	40X-CC-SCRAPS	380.00	??			CN7?	9.7*
718-390	718C		390-460	200	300	105	CN7b-CN7b	9.7-10.3
	718C	41X-1-93-97	390.23	20				
	718C	41X-CC-30-35	399.02	20				
	718C	42X-CC-13-19	400.65	20				
	718C	43X-1-58-62	408.88	20				
	718C	44X-1-48-52	418.28	20				
	718C	46X-1-103-108	437.87	20				
	718C	47X-CC-29-34	448.27	20				
	718C	48X-1-15-20	455.95	20				
	718C	48X-CC-PALEO	456.50	40				

Appendix A (continued).

SAMPLE#	SITE	SAMPLES	DEPTH (mbsl)	VOLUME (cc)	INITIAL DRY WEIGHT (g)	>63 um WEIGHT (g)	NANNOFOSSIL ZONE	DEPOSITIONAL AGE (Ma)
718-460	718C		460-560	160	425	160	CN7b-CN6?	10.3-10.8
	718C	49X-1-33-38	465.63	20				
	718C	52X-1-11-16	493.91	20				
	718C	54X-CC-22-26	514.03	20				
	718C	55X-1-122-126	523.52	20				
	718C	56X-1-69-73	532.49	20				
	718C	56X-4-16-21	536.46	20				
	718C	57X-5-23-28	547.53	20				
	718C	58X-1-40-45	551.20	20				
718-560	718C		560-660	240	460	150	CN6?-CN5b?	10.8-13.0*
	718C	59X-2-78-83	562.58	20				
	718C	59X-4-46-51	565.26	20				
	718C	61X-1-72-76	580.02	20				
	718C	61X-1-110-114	580.40	20				
	718C	61X-2-69-73	581.49	20				
	718C	62X-2-78-83	591.08	20				
	718C	65X-5-119-124	624.49	20				
	718C	66X-1-130-135	628.10	20				
	718C	66X-2-16-20	628.46	20				
	718C	68X-CC-10-14	648.05	20				
	718C	69X-1-7-10	655.37	20				
	718C	69X-1-42-46	655.72	20				
718-660	718C		660-760	220	395	120	CN5b?-CN4?	13.0*-15.7*
	718C	70X-1-48-53	665.16	20				
	718C	70X-1-36-41	665.28	20				
	718C	71X-4-103-108	679.83	20				
	718C	71X-5-43-47	680.73	20				
	718C	72X-2-58-63	685.88	20				
	718C	72X-2-125-130	686.55	20				
	718C	73X-1-136-141	694.66	20				
	718C	73X-2-20-24	695.00	20				
	718C	74X-CC-30-35	704.75	20				
	718C	77X-CC-30-35	731.97	20				
	718C	79X-CC-20-25	754.40	20				
718-760	718C		760-860	240	519	116	CN3/4	15.7*-16.8*
	718C	80X-01-43-47	760.23	20			CN3/4	16.1*
	718C	81X-CC-18-22	772.81	20			CN3	
	718C	82X-01-3-8	778.83	20				
	718C	83X-01-57-61	788.87	20				
	718C	85X-01-43-47	807.73	20				
	718C	86X-01-44-49	817.24	20				
	718C	86X-02-14-19	818.44	20				
	718C	87X-CC-26-31	828.50	20				
	718C	88X-01-37-42	836.17	20				
	718C	89X-01-21-26	845.51	20				
	718C	89X-CC-23-28	846.03	20				
	718C	90X-02-53-57	856.83	20			CN3/4	16.8*
718-860	718C,E		860-960	340	620	162	CN3/4	16.8*-17.2*
	718C	91X-1-39-45	864.68	40			CN3/4	16.8*
	718C	93X-1-11-17	878.11	40				
	718C	93X-CC-20-24	878.79	20				
	718C	95X-1-6-11	897.06	20				
	718C	96X-CC-17-23	906.97	40				
	718C	97X-1-9-11	916.09	20				
	718C	97X-1-36-40	916.25	20				
	718C	98X-CC-5-9	925.55	20				
	718E	2R-3-69-75	942.75	40				
	718E	2R-3-94-100	943.54	40				
	718E	2R-3-130-136	943.90	40			CN3/4	17.2*

APPENDIX B

Fission-track Age Determinations

Individual age determinations were calculated using the equation:

$$t = \frac{1}{\lambda_d} \ln \left[1 + \frac{\lambda_d \zeta \rho_s \rho_d}{2\rho_i} \right] \quad \text{(B.1)}$$

where: t = apatite fission-track age
λ_d = total decay constant for ^{238}U
ζ = the zeta calibration factor
ρ_s = the density of spontaneous tracks
ρ_i = the density of induced tracks
ρ_d = the density of tracks in the fluence monitors

The total decay constant for ^{238}U (λ_d) used is 1.551×10^{-10} yr^{-1}. As discussed in the text, the zeta calibration factor (ζ) was determined to be 322 ± 20 yr/(tracks·cm^2). In practice, because equivalent sized counting areas are used, the ratio N_s/N_i was substituted for ρ_s/ρ_i, where N_s = the number of spontaneous tracks counted and N_i = the number of induced tracks counted in the mica. For the density of tracks in the fluence monitors (ρ_d), the mean value of 2.961×10^6 tracks/cm^2 is used as no fluence gradients were detected in the reactor tubes.

This appendix contains data tables for the determination of fission-track ages of thirty individual apatite grains per dated samples. On each table the following information is given:

Sample—the first digit corresponds to the last digit of the Site number (7 = Site 717, 8 = Site 718), digits following the hypen correspond to the depth (mbsf) to the top of the sampled interval.

NS = number of spontaneous tracks counted (N_s)

NI = number of induced tracks counted (N_i)

Ratio = the ratio of spontaneous and induced tracks counted (N_s/N_i)

Area Units = number of microscopic grid units in which tracks were counted, where one unit counting area is equal to 8.551×10^{-7} cm^2

Rho S = density of spontaneous tracks (tracks/cm^2)

Rho I = density of induced tracks (tracks/cm^2)

Age = single apatite grain fission-track age (Ma)

95% C.I. = the 95% confidence interval of the age determination (m.y.)

Methods used for calculating confidence intervals for single-grain ages, mean (pooled) sample ages, and weighted-mean samples ages are given below:

(i) for single-grain age determinations of 95% C.I. = 1.96 σ, where:

$$\sigma = t \left[\frac{1}{N_s} + \frac{1}{N_i} + \frac{1}{N_d} + \frac{\sigma_\zeta^2}{\zeta^2} \right]^{1/2} \quad \text{(B.2)}$$

and:
t = fission-track age
N_s = number of spontaneous tracks counted
N_i = number of induced tracks counted
N_d = number of induced tracks counted in the mica detectors covering the fluence monitors (N_d = 10183)
ζ = mean of the zeta calibration factor determinations
σ_ζ = standard deviation about the mean zeta

For grains with 0 ages (no spontaneous tracks observed) uncertainties were calculated by taking the uncertainty had a single spontaneous track been observed.

(ii) for mean (pooled) sample ages the 95% C.I. = 1.96σ, where σ is given by equation B.2 also, but here:

$N_s = \Sigma N_s$, total number of spontaneous tracks counted for all grains

$N_i = \Sigma N_i$, total number of induced tracks counted for all grains

where the mean (pooled) age is given by substituting $\Sigma N_s/\Sigma N_i$ for σ_s/σ_i in equation B.1.

(iii) for weighted-mean sample ages the 95% C.I. = $1.96\sigma(n)^{-1/2}$, where the mean and standard deviation are given by:

$$\bar{t} = \frac{\sum \frac{t_i}{\sigma_i^2}}{\sum \frac{1}{\sigma_i^2}} \quad \text{(B.3)}$$

$$\sigma = \left[\frac{n \Sigma \frac{(t_i - \bar{t})^2}{\sigma_i^2}}{(n-1) \Sigma \frac{1}{\sigma_i^2}} \right]^{1/2} \quad \text{(B.4)}$$

where:
t_i = fission-track age of i-th grain
$\bar{t}$ = weighted mean of the individual grain ages
σ_i = standard deviation about the fission track age of the i-th grain (equation B.2)
n = the number of grains for which ages were determined.

Also reported is the chi-squared (χ^2) value (Galbraith, 1980; Green, 1981), which tests the hypothesis that the spread in single grain ages may be solely due to Poisson fluctuation of radioactive decay. The probability of exceeding the χ^2 value for various levels of confidence is found from the reduced chi-squared value (χ_υ^2) given by:

$$\chi_\upsilon^2 = \frac{\chi^2}{\upsilon} \quad \text{(B.5)}$$

where υ = the number of degrees of freedom. Green (1981) suggests that a 5% probability of equaling or exceeding χ^2 be taken as the cut-off for testing the hypothesis that the distribution of ages in a sample are derived from a single population (i.e., single-aged source terranes). For samples dated in this study, υ = 29, and at the 5% level the reduced chi-squared value (χ_υ^2) is 1.47 (Bevington, 1969). Thus, all samples except 7-0, and 8-460, pass the χ^2 test at this level. Green (1981) has suggested taking the unweighted-mean age as being more representative for samples that fail the χ^2 test. We feel that the weighted-mean age given by equation B.3 is more representative in this case as it accounts for the uncertainty associated with single-grain age determinations. For consistency we use the mean (pooled) age for all samples; however, we also report the weighted-mean age in Appendix B. The uncertainties associated with either sample age calculation method overlap for all cases; thus, the use of either age would not significantly alter the interpretations presented.

SAMPLE: 7-0

Grain	NS	NI	Area Units	Ratio	Rho S	Rho I	Age (Ma)	95% C.I. (m.y.)
1	6	398	90	0.0151	7.80E+04	5.17E+06	7.2	5.8
2	2	274	100	0.0073	2.34E+04	3.20E+06	3.5	4.8
3	1	88	36	0.0114	3.25E+04	2.86E+06	5.4	10.7
4	5	169	81	0.0296	7.22E+04	2.44E+06	14.1	12.6
5	3	209	90	0.0144	3.90E+04	2.72E+06	6.8	7.8
6	5	484	90	0.0103	6.50E+04	6.29E+06	4.9	4.3
7	4	298	90	0.0134	5.20E+04	3.87E+06	6.4	6.3
8	0	199	80	0.0000	0.00E+00	2.91E+06	0.0	4.7
9	0	120	100	0.0000	0.00E+00	1.40E+06	0.0	7.8
10	6	111	70	0.0541	1.00E+05	1.85E+06	25.7	21.2
11	4	318	72	0.0126	6.50E+04	5.17E+06	6.0	5.9
12	0	86	90	0.0000	0.00E+00	1.12E+06	0.0	10.9
13	3	260	80	0.0115	4.39E+04	3.80E+06	5.5	6.3
14	3	188	90	0.0160	3.90E+04	2.44E+06	7.6	8.7
15	1	555	80	0.0018	1.46E+04	8.11E+06	0.9	1.7
16	2	540	90	0.0037	2.60E+04	7.02E+06	1.8	2.5
17	3	560	100	0.0054	3.51E+04	6.55E+06	2.6	2.9
18	1	117	25	0.0085	4.68E+04	5.47E+06	4.1	8.0
19	5	282	64	0.0177	9.14E+04	5.15E+06	8.4	7.5
20	2	77	90	0.0260	2.60E+04	1.00E+06	12.4	17.4
21	2	62	100	0.0323	2.34E+04	7.25E+05	15.4	21.6
22	3	284	100	0.0106	3.51E+04	3.32E+06	5.0	5.7
23	0	170	100	0.0000	0.00E+00	1.99E+06	0.0	5.5
24	3	378	90	0.0079	3.90E+04	4.91E+06	3.8	4.3
25	0	249	100	0.0000	0.00E+00	2.91E+06	0.0	3.8
26	2	186	42	0.0108	5.57E+04	5.18E+06	5.1	7.1
27	2	328	100	0.0061	2.34E+04	3.84E+06	2.9	4.0
28	1	158	100	0.0063	1.17E+04	1.85E+06	3.0	5.9
29	9	517	100	0.0174	1.05E+05	6.05E+06	8.3	5.5
30	1	252	100	0.0040	1.17E+04	2.95E+06	1.9	3.7
	79	7917	2540	0.0100			4.8	1.1

Chi-squared value = 56.20 Reduced chi-squared value = 1.94 for 29 degrees of freedom

mean (pooled) age = 4.8 Ma 95% C. I. = 1.1 m.y.
weighted-mean age = 2.7 Ma 95% C. I. = 1.0 m.y.

SAMPLE: 7-220

Grain	NS	NI	Area Units	Ratio	Rho S	Rho I	Age (Ma)	95% C.I. (m.y.)
1	2	181	80	0.0110	2.92E+04	2.65E+06	5.3	7.3
2	3	242	100	0.0124	3.51E+04	2.83E+06	5.9	6.7
3	2	92	70	0.0217	3.34E+04	1.54E+06	10.4	14.5
4	1	231	64	0.0043	1.83E+04	4.22E+06	2.1	4.1
5	0	96	80	0.0000	0.00E+00	1.40E+06	0.0	9.8
6	2	75	40	0.0267	5.85E+04	2.19E+06	12.7	17.9
7	2	93	56	0.0215	4.18E+04	1.94E+06	10.2	14.4
8	6	203	68	0.0296	1.03E+05	3.49E+06	14.1	11.5
9	3	280	56	0.0107	6.26E+04	5.85E+06	5.1	5.8
10	3	291	56	0.0103	6.26E+04	6.08E+06	4.9	5.6
11	8	369	54	0.0217	1.73E+05	7.99E+06	10.3	7.3
12	2	116	100	0.0172	2.34E+04	1.36E+06	8.2	11.5
13	1	106	70	0.0094	1.67E+04	1.77E+06	4.5	8.9
14	2	166	72	0.0120	3.25E+04	2.70E+06	5.7	8.0
15	2	126	100	0.0159	2.34E+04	1.47E+06	7.6	10.6
16	1	117	100	0.0085	1.17E+04	1.37E+06	4.1	8.0
17	5	272	90	0.0184	6.50E+04	3.53E+06	8.8	7.8
18	2	228	70	0.0088	3.34E+04	3.81E+06	4.2	5.8
19	3	310	66	0.0097	5.32E+04	5.49E+06	4.6	5.3
20	0	157	100	0.0000	0.00E+00	1.84E+06	0.0	6.0
21	4	112	50	0.0357	9.36E+04	2.62E+06	17.0	17.0
22	1	158	70	0.0063	1.67E+04	2.64E+06	3.0	5.9
23	2	148	80	0.0135	2.92E+04	2.16E+06	6.4	9.0
24	2	89	25	0.0225	9.36E+04	4.16E+06	10.7	15.0
25	1	314	100	0.0032	1.17E+04	3.67E+06	1.5	3.0
26	5	176	80	0.0284	7.31E+04	2.57E+06	13.5	12.1
27	2	91	70	0.0220	3.34E+04	1.52E+06	10.5	14.7
28	4	231	60	0.0173	7.80E+04	4.50E+06	8.2	8.2
29	4	147	60	0.0272	7.80E+04	2.87E+06	13.0	12.9
30	1	181	50	0.0055	2.34E+04	4.23E+06	2.6	5.2
	76	5398	2137	0.0141			6.7	1.6

Chi-squared value = 27.07 Reduced chi-squared value = 0.93 for 29 degrees of freedom

mean (pooled) age = 6.7 Ma 95% C. I. = 1.6 m.y.
weighted-mean age = 4.5 Ma 95% C. I. = 1.2 m.y.

Appendix B (continued).

SAMPLE: 7-420

Grain	NS	NI	Area Units	Ratio	Rho S	Rho I	Age (Ma)	95% C.I. (m.y.)
1	5	355	100	0.0141	5.85E+04	4.15E+06	6.7	5.9
2	17	554	100	0.0307	1.99E+05	6.48E+06	14.6	7.1
3	1	110	80	0.0091	1.46E+04	1.61E+06	4.3	8.5
4	1	97	60	0.0103	1.95E+04	1.89E+06	4.9	9.7
5	10	362	40	0.0276	2.92E+05	1.06E+07	13.2	8.3
6	9	587	100	0.0153	1.05E+05	6.86E+06	7.3	4.8
7	3	203	72	0.0148	4.87E+04	3.30E+06	7.0	8.0
8	2	174	45	0.0115	5.20E+04	4.52E+06	5.5	7.6
9	2	134	100	0.0149	2.34E+04	1.57E+06	7.1	9.9
10	5	222	35	0.0225	1.67E+05	7.42E+06	10.7	9.5
11	2	118	85	0.0169	2.75E+04	1.62E+06	8.1	11.3
12	7	227	35	0.0308	2.34E+05	7.58E+06	14.7	11.1
13	1	170	70	0.0059	1.67E+04	2.84E+06	2.8	5.5
14	0	24	90	0.0000	0.00E+00	3.12E+05	0.0	39.7
15	3	302	80	0.0099	4.39E+04	4.41E+06	4.7	5.4
16	8	694	100	0.0115	9.36E+04	8.12E+06	5.5	3.8
17	4	135	100	0.0296	4.68E+04	1.58E+06	14.1	14.1
18	0	134	80	0.0000	0.00E+00	1.96E+06	0.0	7.0
19	8	215	100	0.0372	9.36E+04	2.51E+06	17.7	12.5
20	4	297	64	0.0135	7.31E+04	5.43E+06	6.4	6.3
21	8	179	50	0.0447	1.87E+05	4.19E+06	21.3	15.1
22	6	333	100	0.0180	7.02E+04	3.89E+06	8.6	7.0
23	11	445	100	0.0247	1.29E+05	5.20E+06	11.8	7.1
24	7	447	80	0.0157	1.02E+05	6.53E+06	7.5	5.6
25	5	182	50	0.0275	1.17E+05	4.26E+06	13.1	11.7
26	2	135	50	0.0148	4.68E+04	3.16E+06	7.1	9.9
27	2	152	50	0.0132	4.68E+04	3.56E+06	6.3	8.8
28	2	140	56	0.0143	4.18E+04	2.92E+06	6.8	9.5
29	3	113	60	0.0265	5.85E+04	2.20E+06	12.6	14.5
30	5	293	70	0.0171	8.35E+04	4.89E+06	8.1	7.2
	143	7533	2202	0.0190			9.0	1.6

Chi-squared value = 30.97 Reduced chi-squared value = 1.07 for 29 degrees of freedom

mean (pooled) age = 9.0 Ma 95% C. I. = 1.6 m.y.
weighted-mean age = 7.3 Ma 95% C. I. = 1.3 m.y.

SAMPLE: 7-620

Grain	NS	NI	Area Units	Ratio	Rho S	Rho I	Age (Ma)	95% C.I. (m.y.)
1	9	263	60	0.0342	1.75E+05	5.13E+06	16.3	10.9
2	4	219	100	0.0183	4.68E+04	2.56E+06	8.7	8.6
3	1	121	60	0.0083	1.95E+04	2.36E+06	3.9	7.8
4	6	225	50	0.0267	1.40E+05	5.26E+06	12.7	10.3
5	4	139	50	0.0288	9.36E+04	3.25E+06	13.7	13.6
6	7	152	90	0.0461	9.10E+04	1.98E+06	21.9	16.7
7	7	275	100	0.0255	8.19E+04	3.22E+06	12.1	9.1
8	0	81	100	0.0000	0.00E+00	9.47E+05	0.0	11.6
9	7	363	100	0.0193	8.19E+04	4.25E+06	9.2	6.9
10	9	323	100	0.0279	1.05E+05	3.78E+06	13.3	8.8
11	1	46	64	0.0217	1.83E+04	8.41E+05	10.4	20.5
12	2	127	54	0.0157	4.33E+04	2.75E+06	7.5	10.5
13	3	73	60	0.0411	5.85E+04	1.42E+06	19.6	22.6
14	3	197	100	0.0152	3.51E+04	2.30E+06	7.3	8.3
15	6	246	72	0.0244	9.75E+04	4.00E+06	11.6	9.4
16	4	209	90	0.0191	5.20E+04	2.72E+06	9.1	9.0
17	9	412	100	0.0218	1.05E+05	4.82E+06	10.4	6.9
18	5	219	50	0.0228	1.17E+05	5.12E+06	10.9	9.7
19	6	304	100	0.0197	7.02E+04	3.56E+06	9.4	7.6
20	2	63	100	0.0317	2.34E+04	7.37E+05	15.1	21.3
21	1	82	50	0.0122	2.34E+04	1.92E+06	5.8	11.5
22	4	86	60	0.0465	7.80E+04	1.68E+06	22.1	22.2
23	12	319	90	0.0376	1.56E+05	4.15E+06	17.9	10.4
24	14	421	100	0.0333	1.64E+05	4.92E+06	15.8	8.5
25	5	158	100	0.0316	5.85E+04	1.85E+06	15.1	13.4
26	10	248	60	0.0403	1.95E+05	4.83E+06	19.2	12.2
27	1	70	100	0.0143	1.17E+04	8.19E+05	6.8	13.4
28	7	348	100	0.0201	8.19E+04	4.07E+06	9.6	7.2
29	9	467	100	0.0193	1.05E+05	5.46E+06	9.2	6.1
30	5	267	100	0.0187	5.85E+04	3.12E+06	8.9	7.9
	163	6523	2460	0.0250			11.9	2.0

Chi-squared value = 20.01 Reduced chi-squared value = 0.69 for 29 degrees of freedom

mean (pooled) age = 11.9 Ma 95% C. I. = 2.0 m.y.
weighted-mean age = 10.5 Ma 95% C. I. = 1.5 m.y.

Appendix B (continued).

SAMPLE: 7-720

Grain	NS	NI	Area Units	Ratio	Rho S	Rho I	Age (Ma)	95% C.I. (m.y.)
1	9	452	70	0.0199	1.50E+05	7.55E+06	9.5	6.3
2	5	209	36	0.0239	1.62E+05	6.79E+06	11.4	10.1
3	9	247	40	0.0364	2.63E+05	7.22E+06	17.3	11.6
4	14	448	60	0.0313	2.73E+05	8.73E+06	14.9	8.0
5	6	195	70	0.0308	1.00E+05	3.26E+06	14.7	11.9
6	8	421	100	0.0190	9.36E+04	4.92E+06	9.1	6.4
7	6	273	70	0.0220	1.00E+05	4.56E+06	10.5	8.5
8	9	308	50	0.0292	2.11E+05	7.20E+06	13.9	9.3
9	14	351	64	0.0399	2.56E+05	6.41E+06	19.0	10.2
10	2	91	40	0.0220	5.85E+04	2.66E+06	10.5	14.7
11	14	447	100	0.0313	1.64E+05	5.23E+06	14.9	8.0
12	7	202	70	0.0347	1.17E+05	3.37E+06	16.5	12.5
13	5	115	100	0.0435	5.85E+04	1.34E+06	20.7	18.6
14	7	122	35	0.0574	2.34E+05	4.08E+06	27.3	20.9
15	7	164	100	0.0427	8.19E+04	1.92E+06	20.3	15.4
16	3	38	50	0.0789	7.02E+04	8.89E+05	37.5	44.2
17	6	254	64	0.0236	1.10E+05	4.64E+06	11.3	9.1
18	2	64	35	0.0313	6.68E+04	2.14E+06	14.9	21.0
19	11	436	100	0.0252	1.29E+05	5.10E+06	12.0	7.2
20	5	185	80	0.0270	7.31E+04	2.70E+06	12.9	11.5
21	3	53	100	0.0566	3.51E+04	6.20E+05	26.9	31.4
22	4	119	100	0.0336	4.68E+04	1.39E+06	16.0	16.0
23	3	119	100	0.0252	3.51E+04	1.39E+06	12.0	13.8
24	1	37	80	0.0270	1.46E+04	5.41E+05	12.9	25.6
25	3	117	50	0.0256	7.02E+04	2.74E+06	12.2	14.0
26	5	151	100	0.0331	5.85E+04	1.77E+06	15.8	14.1
27	8	237	80	0.0338	1.17E+05	3.46E+06	16.1	11.4
28	5	175	30	0.0286	1.95E+05	6.82E+06	13.6	12.1
29	8	235	100	0.0340	9.36E+04	2.75E+06	16.2	11.5
30	5	199	80	0.0251	7.31E+04	2.91E+06	12.0	10.6
	194	6464	2154	0.0300			14.3	2.2

Chi-squared value = 15.58 Reduced chi-squared value = 0.54 for 29 degrees of freedom

mean (pooled) age = 14.3 Ma 95% C. I. = 2.2 m.y.
weighted-mean age = 13.3 Ma 95% C. I. = 1.3 m.y.

SAMPLE: 8-290

Grain	NS	NI	Area Units	Ratio	Rho S	Rho I	Age (Ma)	95% C.I. (m.y.)
1	11	273	45	0.0403	2.86E+05	7.09E+06	19.2	11.6
2	2	163	100	0.0123	2.34E+04	1.91E+06	5.8	8.2
3	1	26	25	0.0385	4.68E+04	1.22E+06	18.3	36.6
4	29	491	100	0.0591	3.39E+05	5.74E+06	28.1	10.7
5	9	221	50	0.0407	2.11E+05	5.17E+06	19.4	13.0
6	6	218	60	0.0275	1.17E+05	4.25E+06	13.1	10.7
7	3	96	50	0.0313	7.02E+04	2.25E+06	14.9	17.1
8	14	603	100	0.0232	1.64E+05	7.05E+06	11.1	5.9
9	2	35	50	0.0571	4.68E+04	8.19E+05	27.2	38.8
10	3	137	50	0.0219	7.02E+04	3.20E+06	10.4	11.9
11	8	234	100	0.0342	9.36E+04	2.74E+06	16.3	11.5
12	8	229	100	0.0349	9.36E+04	2.68E+06	16.6	11.8
13	2	167	100	0.0120	2.34E+04	1.95E+06	5.7	8.0
14	19	476	100	0.0399	2.22E+05	5.57E+06	19.0	8.8
15	3	151	72	0.0199	4.87E+04	2.45E+06	9.5	10.8
16	6	100	72	0.0600	9.75E+04	1.62E+06	28.5	23.6
17	7	195	32	0.0359	2.56E+05	7.13E+06	17.1	12.9
18	7	403	90	0.0174	9.10E+04	5.24E+06	8.3	6.2
19	6	103	36	0.0583	1.95E+05	3.35E+06	27.7	22.9
20	9	473	90	0.0190	1.17E+05	6.15E+06	9.1	6.0
21	9	268	100	0.0336	1.05E+05	3.13E+06	16.0	10.7
22	11	374	100	0.0294	1.29E+05	4.37E+06	14.0	8.4
23	2	117	100	0.0171	2.34E+04	1.37E+06	8.1	11.4
24	13	427	100	0.0304	1.52E+05	4.99E+06	14.5	8.1
25	2	44	100	0.0455	2.34E+04	5.15E+05	21.6	30.7
26	12	307	90	0.0391	1.56E+05	3.99E+06	18.6	10.8
27	14	369	70	0.0379	2.34E+05	6.16E+06	18.1	9.7
28	4	138	60	0.0290	7.80E+04	2.69E+06	13.8	13.7
29	3	65	80	0.0462	4.39E+04	9.50E+05	22.0	25.5
30	22	346	60	0.0636	4.29E+05	6.74E+06	30.2	13.2
	247	7249	2282	0.0341			16.2	2.3

Chi-squared value = 38.92 Reduced chi-squared value = 1.34 for 29 degrees of freedom

mean (pooled) age = 16.2 Ma 95% C. I. = 2.3 m.y.
weighted-mean age = 13.5 Ma 95% C. I. = 2.2 m.y.

Appendix B (continued).

SAMPLE: 8-460

Grain	NS	NI	Area Units	Ratio	Rho S	Rho I	Age (Ma)	95% C.I. (m.y.)
1	32	79	72	0.4051	5.20E+05	1.28E+06	190.3	79.0
2	1	59	100	0.0169	1.17E+04	6.90E+05	8.1	16.0
3	4	102	50	0.0392	9.36E+04	2.39E+06	18.7	18.7
4	4	78	72	0.0513	6.50E+04	1.27E+06	24.4	24.6
5	6	148	100	0.0405	7.02E+04	1.73E+06	19.3	15.8
6	5	133	40	0.0376	1.46E+05	3.89E+06	17.9	16.0
7	16	418	80	0.0383	2.34E+05	6.11E+06	18.2	9.2
8	17	422	90	0.0403	2.21E+05	5.48E+06	19.2	9.4
9	7	126	10	0.0556	8.19E+05	1.47E+07	26.4	20.2
10	8	419	100	0.0191	9.36E+04	4.90E+06	9.1	6.4
11	5	141	10	0.0355	5.85E+05	1.65E+07	16.9	15.1
12	2	53	90	0.0377	2.60E+04	6.89E+05	18.0	25.4
13	19	232	100	0.0819	2.22E+05	2.71E+06	38.9	18.4
14	9	176	100	0.0511	1.05E+05	2.06E+06	24.3	16.4
15	8	325	100	0.0246	9.36E+04	3.80E+06	11.7	8.3
16	11	281	40	0.0391	3.22E+05	8.22E+06	18.6	11.3
17	13	249	30	0.0522	5.07E+05	9.71E+06	24.8	13.9
18	18	461	90	0.0390	2.34E+05	5.99E+06	18.6	8.8
19	8	185	100	0.0432	9.36E+04	2.16E+06	20.6	14.6
20	3	46	90	0.0652	3.90E+04	5.98E+05	31.0	36.3
21	6	140	50	0.0429	1.40E+05	3.27E+06	20.4	16.7
22	4	209	60	0.0191	7.80E+04	4.07E+06	9.1	9.0
23	11	236	60	0.0466	2.14E+05	4.60E+06	22.2	13.5
24	5	187	50	0.0267	1.17E+05	4.37E+06	12.7	11.3
25	11	351	90	0.0313	1.43E+05	4.56E+06	14.9	9.0
26	13	276	60	0.0471	2.53E+05	5.38E+06	22.4	12.5
27	5	259	100	0.0193	5.85E+04	3.03E+06	9.2	8.2
28	20	213	50	0.0939	4.68E+05	4.98E+06	44.6	20.6
29	1	80	70	0.0125	1.67E+04	1.34E+06	6.0	11.8
30	4	150	70	0.0267	6.68E+04	2.51E+06	12.7	12.6
	276	6234	2124	0.0443			21.1	2.9

Chi-squared value = 207.39 Reduced chi-squared value = 7.15 for 29 degrees of freedom

mean (pooled) age = 21.1 Ma 95% C. I. = 2.9 m.y.
weighted-mean age = 15.9 Ma 95% C. I. = 3.1 m.y.

SAMPLE: 8-660

Grain	NS	NI	Area Units	Ratio	Rho S	Rho I	Age (Ma)	95% C.I. (m.y.)
1	9	230	90	0.0391	1.17E+05	2.99E+06	18.6	12.5
2	1	82	42	0.0122	2.78E+04	2.28E+06	5.8	11.5
3	4	58	63	0.0690	7.43E+04	1.08E+06	32.8	33.3
4	3	26	80	0.1154	4.39E+04	3.80E+05	54.8	65.5
5	6	172	32	0.0349	2.19E+05	6.29E+06	16.6	13.6
6	8	99	100	0.0808	9.36E+04	1.16E+06	38.4	27.8
7	19	716	100	0.0265	2.22E+05	8.37E+06	12.6	5.8
8	3	78	81	0.3385	4.33E+04	1.13E+06	18.3	21.1
9	15	317	45	0.0473	3.90E+05	8.24E+06	22.5	11.7
10	10	347	100	0.0288	1.17E+05	4.06E+06	13.7	8.7
11	9	302	81	0.0298	1.30E+05	4.36E+06	14.2	9.4
12	15	307	45	0.0489	3.90E+05	7.98E+06	23.3	12.1
13	4	23	24	0.1739	1.95E+05	1.12E+06	82.4	87.6
14	7	253	49	0.0277	1.67E+05	6.04E+06	13.2	9.9
15	11	368	80	0.0299	1.61E+05	5.38E+06	14.2	8.6
16	2	87	90	0.0230	2.60E+04	1.13E+06	10.9	15.4
17	5	229	63	0.0218	9.28E+04	4.25E+06	10.4	9.2
18	3	164	48	0.0183	7.31E+04	4.00E+06	8.7	10.0
19	2	51	90	0.0392	2.60E+04	6.63E+05	18.7	26.4
20	7	185	142	0.0378	5.76E+04	1.52E+06	18.0	13.6
21	21	345	80	0.0609	3.07E+05	5.04E+06	29.0	12.9
22	12	417	80	0.0288	1.75E+05	6.10E+06	13.7	7.9
23	6	125	50	0.0480	1.40E+05	2.92E+06	22.8	18.8
24	6	123	50	0.0488	1.40E+05	2.88E+06	23.2	19.1
25	13	317	90	0.0410	1.69E+05	4.12E+06	19.5	10.9
26	4	87	40	0.0460	1.17E+05	2.54E+06	21.9	22.0
27	9	242	50	0.0372	2.11E+05	5.66E+06	17.7	11.8
28	7	172	70	0.0407	1.17E+05	2.87E+06	19.4	14.7
29	30	600	100	0.0500	3.51E+05	7.02E+06	23.8	8.8
30	8	177	100	0.0452	9.36E+04	2.07E+06	21.5	15.3
	259	6699	2155	0.0387			18.4	2.6

Chi-squared value = 38.74 Reduced chi-squared value = 1.34 for 29 degrees of freedom

mean (pooled) age = 18.4 Ma 95% C. I. = 2.6 m.y.
weighted-mean age = 16.1 Ma 95% C. I. = 2.1 m.y.

Appendix B (continued).

SAMPLE: 8-760

Grain	NS	NI	Area Units	Ratio	Rho S	Rho I	Age (Ma)	95% C.I. (m.y.)
1	3	81	25	0.0370	1.40E+05	3.79E+06	17.6	20.3
2	9	256	80	0.0352	1.32E+05	3.74E+06	16.7	11.2
3	10	468	100	0.0214	1.17E+05	5.47E+06	10.2	6.4
4	4	120	45	0.0333	1.04E+05	3.12E+06	15.9	15.8
5	8	218	50	0.0367	1.87E+05	5.10E+06	17.5	12.4
6	3	67	40	0.0448	8.77E+04	1.96E+06	21.3	24.7
7	8	171	50	0.0468	1.87E+05	4.00E+06	22.3	15.8
8	13	272	70	0.0478	2.17E+05	4.54E+06	22.7	12.7
9	10	287	60	0.0348	1.95E+05	5.59E+06	16.6	10.5
10	4	156	100	0.0256	4.68E+04	1.82E+06	12.2	12.1
11	2	29	50	0.0690	4.68E+04	6.78E+05	32.8	47.0
12	3	125	35	0.0240	1.00E+05	4.18E+06	11.4	13.1
13	8	146	30	0.0548	3.12E+05	5.69E+06	26.1	18.6
14	4	143	48	0.0280	9.75E+04	3.48E+06	13.3	13.3
15	9	136	30	0.0662	3.51E+05	5.30E+06	31.5	21.3
16	3	71	49	0.0423	7.16E+04	1.69E+06	20.1	23.3
17	14	280	72	0.0500	2.27E+05	4.55E+06	23.8	12.9
18	4	102	32	0.0392	1.46E+05	3.73E+06	18.7	18.7
19	3	57	56	0.0526	6.26E+04	1.19E+06	25.0	29.1
20	15	375	80	0.0400	2.19E+05	5.48E+06	19.0	9.9
21	2	62	64	0.0323	3.65E+04	1.13E+06	15.4	21.6
22	11	319	100	0.0345	1.29E+05	3.73E+06	16.4	9.9
23	3	92	35	0.0326	1.00E+05	3.07E+06	15.5	17.9
24	5	131	24	0.0382	2.44E+05	6.38E+06	18.2	16.3
25	8	142	35	0.0563	2.67E+05	4.74E+06	26.8	19.2
26	3	46	50	0.0652	7.02E+04	1.08E+06	31.0	36.3
27	3	101	40	0.0297	8.77E+04	2.95E+06	14.1	16.3
28	7	142	30	0.0493	2.73E+05	5.54E+06	23.5	17.9
29	2	49	60	0.0408	3.90E+04	9.55E+05	19.4	27.5
30	3	81	24	0.0370	1.46E+05	3.95E+06	17.6	20.3
	184	4725	1564	0.0389			18.5	3.0

Chi-squared value = 14.44 Reduced chi-squared value = 0.50 for 29 degrees of freedom

mean (pooled) age = 18.5 Ma 95% C. I. = 3.0 m.y.
weighted-mean age = 17.0 Ma 95% C. I. = 1.8 m.y.

SAMPLE: 8-860

Grain	NS	NI	Area Units	Ratio	Rho S	Rho I	Age (Ma)	95% C.I. (m.y.)
1	11	205	56	0.0537	2.30E+05	4.28E+06	25.5	15.6
2	4	191	50	0.0209	9.36E+04	4.47E+06	10.0	9.9
3	8	225	63	0.0356	1.49E+05	4.18E+06	16.9	12.0
4	16	438	81	0.0365	2.31E+05	6.32E+06	17.4	8.7
5	5	311	50	0.0161	1.17E+05	7.27E+06	7.7	6.8
6	6	112	60	0.0536	1.17E+05	2.18E+06	25.5	21.0
7	13	311	63	0.0418	2.41E+05	5.77E+06	19.9	11.1
8	4	162	100	0.0247	4.68E+04	1.89E+06	11.8	11.7
9	8	259	90	0.0309	1.04E+05	3.37E+06	14.7	10.4
10	6	318	80	0.0189	8.77E+04	4.65E+06	9.0	7.3
11	7	248	81	0.0282	1.01E+05	3.58E+06	13.4	10.1
12	3	87	50	0.0345	7.02E+04	2.03E+06	16.4	18.9
13	3	59	50	0.0508	7.02E+04	1.38E+06	24.2	28.1
14	1	31	56	0.0323	2.09E+04	6.47E+05	15.4	30.6
15	9	241	50	0.0373	2.11E+05	5.64E+06	17.8	11.9
16	5	98	81	0.0510	7.22E+04	1.41E+06	24.3	21.9
17	3	57	40	0.0526	8.77E+04	1.67E+06	25.0	29.1
18	9	296	48	0.0304	2.19E+05	7.21E+06	14.5	9.6
19	15	409	100	0.0367	1.75E+05	4.78E+06	17.5	9.1
20	4	97	50	0.0412	9.36E+04	2.27E+06	19.6	19.7
21	5	203	54	0.0246	1.08E+05	4.40E+06	11.7	10.4
22	8	197	60	0.0406	1.56E+05	3.84E+06	19.3	13.7
23	8	225	64	0.0356	1.46E+05	4.11E+06	16.9	12.0
24	6	296	100	0.0203	7.02E+04	3.46E+06	9.7	7.8
25	12	415	80	0.0289	1.75E+05	6.07E+06	13.8	7.9
26	5	105	54	0.0476	1.08E+05	2.27E+06	22.7	20.4
27	4	143	50	0.0280	9.36E+04	3.34E+06	13.3	13.3
28	6	111	80	0.0541	8.77E+04	1.62E+06	25.7	21.2
29	6	227	60	0.0264	1.17E+05	4.42E+06	12.6	10.2
30	16	420	70	0.0381	2.67E+05	7.02E+06	18.1	9.1
	216	6497	1971	0.0332			15.8	2.4

Chi-squared value = 18.39 Reduced chi-squared value = 0.63 for 29 degrees of freedom

mean (pooled) age = 15.8 Ma 95% C. I. = 2.4 m.y.
weighted-mean age = 14.3 Ma 95% C. I. = 1.7 m.y.

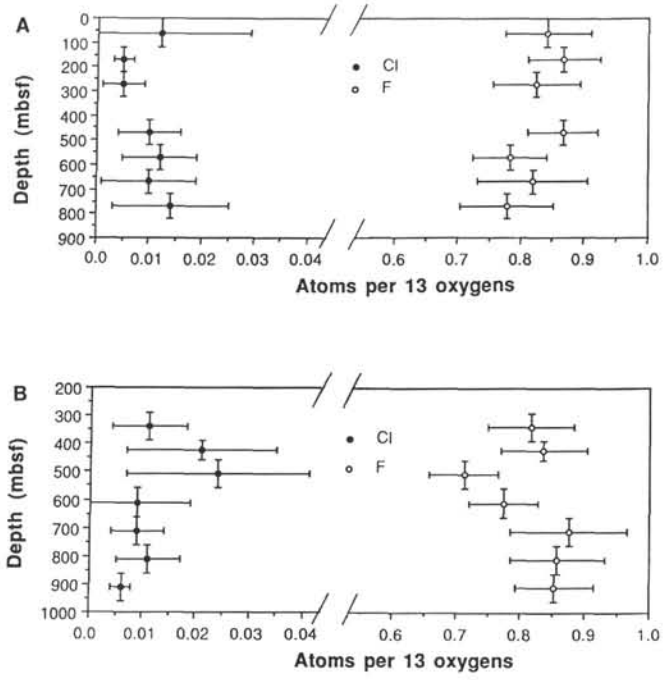

Figure 8. Mean number of Cl and F atoms per apatite molecule, as well as the standard error of the mean (95% confidence interval), for each sample are plotted against depth for **A.** Site 717 holes and **B.** Site 718 holes.

APPENDIX C

Apatite Compositions

Electron microprobe compositional data were determined for 20 randomly chosen apatites per sample to test the hypothesis that track-shortening trends reflect variations in sample-averaged apatite Cl content. CaO, ^{205}P, F, and Cl were analyzed by using the wavelength dispersive system set at a maximum count time of 60 s on a JEOL 733 electron microprobe. Operating conditions were 15 KeV and a 20-nA sample current. A 20-μm beam diameter was used to minimize F burnoff. Avoidance of the 3-P-K_α interference with 1-F-K_α when analyzing for F was achieved by filtering out the higher order phosphorous peak using the single-channel analyzer. All analyses were converted to weight percent using the Bence-Albee reduction scheme. Determined weight percents for each element were converted to number of atoms per 13 oxygens for a $Ca_5(PO_4)_3(OH, F, Cl)$ molecule. The mean number of Cl and F atoms per apatite molecule as well as the standard error of the mean at the 95% confidence interval, for each sample, are plotted versus depth for Site 717 (Fig. 8A) and Site 718 (Fig. 8B) samples. All samples comprise predominantly of F-OH apatites containing on average less than 0.04 atoms of Cl per apatite molecule. No correlation between average anion composition and mean track length is observed. Thus, we conclude that the decrease in mean track length below 560 mbsf at Site 718 is not due to a decrease in apatite Cl content below this depth.